Journal of Biomolecular NMR, **12:** 319–324, 1998.
KLUWER/ESCOM

Rapid measurement of scalar three-bond $^{1}H^{N}$-$^{1}H^{\alpha}$ spin coupling constants in ^{15}N-labelled proteins

Hannes Ponstingl & Gottfried Otting*
Department of Medical Biochemistry and Biophysics, Karolinska Institute, Doktorsringen 9-A1, S-171 77 Stockholm, Sweden

Received 11 February 1998; Accepted 23 March 1998

Key words: scalar three-bond coupling constant, *E. coli* flavodoxin, *E. coli* arginine repressor, differential relaxation, CT-HMQC-HA, CT-HMQC-HN

Abstract

Two new 2D NMR experiments, CT-HMQC-HA and CT-HMQC-HN, are proposed for the rapid measurement of homonuclear $^{3}J_{HNH\alpha}$ coupling constants of uniformly ^{15}N-enriched proteins in solution. The experiments are based on the comparison of the signal intensities in a pair of constant-time [^{15}N,^{1}H]-HMQC spectra recorded with and without decoupling of the amide proton – α proton coupling. Experimental data recorded with the 78-residue N-terminal domain of the *E. coli* arginine repressor (ArgR-N) and with oxidized *E. coli* flavodoxin (176 residues) showed good agreement with $^{3}J_{HNH\alpha}$ coupling constants obtained by fitting of the multiplet fine structure of the amide proton resonances or from a 3D HNHA-J experiment, respectively. Quantitative estimates for the effects from different relaxation rates of in-phase and antiphase magnetization are given.

For small proteins, $^{3}J_{HNH\alpha}$ coupling constants can be determined most efficiently from in-phase multiplets observed, for instance, in homonuclear NOESY spectra or in [^{15}N,^{1}H]-HSQC spectra recorded with a purge pulse (Szyperski et al., 1992). For larger proteins, accurate measurements require more specific techniques like E.COSY-type (Schmieder et al., 1991; Seip et al., 1992; Görlach et al., 1993; Madsen et al., 1993; Weisemann et al., 1994; Löhr and Rüterjans, 1995) or DQ/ZQ experiments (Rexroth et al., 1995). These techniques require, however, doubly ^{13}C/^{15}N-labelled protein samples and usually the recording of 3D spectra. Only the $S^{3}E$ and $S^{3}CT$ experiments (Meissner et al., 1997; Sørensen et al., 1997) can conveniently be recorded as 2D spectra using ^{15}N-labelled protein samples, but require a homonuclear magnetization transfer between the H^{N} and H^{α} protons by NOE or TOCSY mixing. For larger proteins, homonuclear TOCSY transfer is inefficient and NOESY spectra are crowded in the spectral region containing the H^{N}-H^{α} cross peaks. Furthermore, the $^{3}J_{HNH\alpha}$ coupling constants are determined from the relatively broad H^{α} resonances, leading to non-optimal sensitivity and potential interference with t_1 noise from the water resonance.

In a different approach, $^{3}J_{HNH\alpha}$ values are encoded in cross-peak intensities and determined either by a nonlinear fit of peak intensities in a series of J-modulated [^{15}N,^{1}H]-HSQC (Billeter et al., 1992), HMQC (Kay et al., 1989) or constant-time HMQC (Kuboniwa et al., 1994) spectra, or, perhaps simpler, from the intensity ratio of diagonal and cross peaks in a single 3D HNHA-J spectrum (Vuister and Bax, 1993; Kuboniwa et al., 1994). ^{15}N labelling is sufficient for these experiments.

For maximum ease of data evaluation, one might wish for an experiment where the $^{3}J_{HNH\alpha}$ coupling constant could be extracted by simple comparison of the intensities of ^{15}N-^{1}H cross peaks of amide groups observed in not more than two 2D HSQC- or HMQC-type spectra, as the resolution in these spectra is usually good even for larger proteins. Here, two different constant-time experiments, CT-HMQC-HN and CT-HMQC-HA, are proposed to achieve this goal for

*To whom correspondence should be addressed.

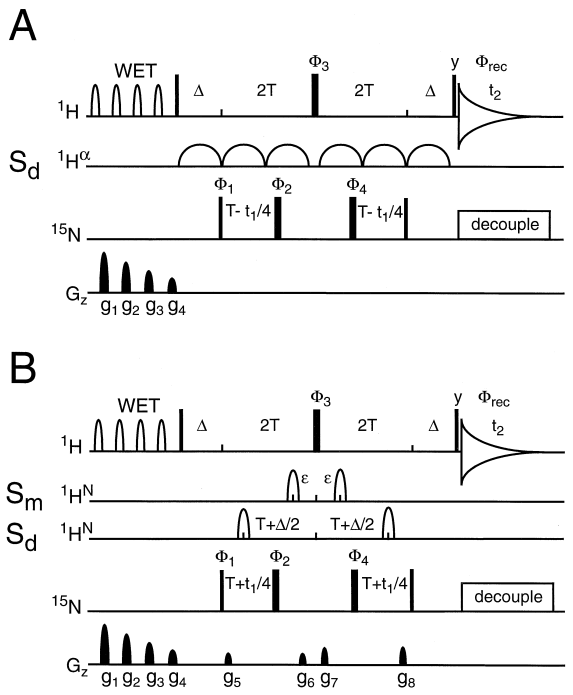

Figure 1. Pulse schemes of the 2D CT-HMQC-HA and CT-HMQC-HN experiments for the measurement of $^3J_{HNH\alpha}$ coupling constants. Narrow and wide bars indicate 90° and 180° pulses, respectively, and round shapes indicate selective pulses. All rf pulses are applied with phase x unless indicated differently. Phase cycle: $\Phi_1 = 64(x)$; $\Phi_2 = 16(x), 16(y), 16(-y), 16(-x)$; $\Phi_3 = 16(x, y, -x, -y)$; $\Phi_4 = 4[4(x), 4(y), 4(-x), 4(-y)]$. $\Phi_{rec} = 2\{2[2(+,-), 2(-,+)], 2[2(-,+), 2(+,-)]\}$. Φ_1 is incremented according to the States-TPPI scheme (Marion et al., 1989). $\Delta = 1/(2^1J_{HN})$. Two data sets, referred to as 'decoupled' (S_d) and 'J-modulated' (S_m), are recorded for each experiment. The water signal was suppressed by a WET sequence (Smallcombe et al., 1995) using selective pulses of 5 ms duration and PFG amplitudes (duration): $g_1 = 2g_2 = 4g_3 = 8g_4 = 32.0$ G/cm (2 ms). (A) CT-HMQC-HA experiment. The data sets S_d and S_m are recorded, respectively, with and without a train of inversion pulses selectively acting on the H^α resonances. Experiments with ArgR-N (flavodoxin) were recorded with hyperbolic secant pulses (Silver et al., 1984) of 5.4 ms duration, inverting the signals in the region 3.9 ± 1.5 ppm (4.0 ± 1.5 ppm), with phase alternation in the pulse train (+, −, −, +). T = 10.8 ms (5.4 ms), $t_{1max} = 31.2$ ms (19.2 ms) and $t_{2max} = 312.2$ ms (114.7 ms). (B) CT-HMQC-HN experiment. The selective pulses during the constant time delay are 180° pulses selectively refocusing the H^N but not the H^α resonances. The J-modulated data set S_m is recorded with short delays ε, each accommodating half the selective refocusing pulse as well as one of the PFGs g_6 and g_7 including eddy-current recovery delay. The decoupled data set S_d is recorded with $\varepsilon = T + \Delta/2$. PFG amplitudes (duration): $2g_5 = 2g_6 = g_7 = g_8 = 7.5$ G/cm (500 μs). Experiments with ArgR-N (flavodoxin) were recorded using RE-BURP (Geen and Freeman, 1991) pulses of 3.5 ms (2.1 ms) duration to refocus the signals in the region 8.0 ± 1.7 ppm (8.8 ± 2.4 ppm); T = 12.0 ms (7.5 ms), $t_{1max} = 28.8$ ms (17.7 ms) and $t_{2max} = 312.2$ ms (114.7 ms). Longer delays T improve the spectral resolution in the ^{15}N dimension and allow for more dephasing under small couplings, but reduce sensitivity due to relaxation. In practice, J-modulation periods between 30 and 70 ms resulted in comparable accuracy of the coupling constants measured both with ArgR-N and flavodoxin.

uniformly ^{15}N-enriched or $^{13}C/^{15}N$ doubly labelled proteins.

Figure 1 shows the pulse sequences of the CT-HMQC-HA and CT-HMQC-HN experiments. They are based on the constant-time [^{15}N,^1H]-HMQC scheme (Kuboniwa et al., 1994), where, starting from amide proton magnetization, heteronuclear two-spin coherence is generated between the amide protons and the directly bonded amide nitrogens. Unless the amide protons are decoupled from the α protons by some means, they evolve under the $^3J_{HNH\alpha}$ coupling during the entire time period $4T + 2\Delta$ between the first and the last non-selective 90°(^1H) pulse (Figure 1). The 90°(^1H) pulse at the end of the pulse sequences converts any amide proton magnetization, which is antiphase with respect to the α protons, into α proton magnetization (Frey et al., 1985). Decoupling between the amide and α protons is achieved either by a train of semi-selective inversion pulses applied to the α protons (CT-HMQC-HA, Figure 1A) or by semi-selective 180° refocusing pulses applied to the amide protons in the middle of each time period $2T + \Delta$ (CT-HMQC-HN, Figure 1B). 'J-modulated' spectra are obtained by omitting the selective decoupling pulse train (CT-HMQC-HA, Figure 1A) or by shifting the selective 180° refocusing pulses close to the central non-selective 180°(^1H) pulse (CT-HMQC-HN, Figure 1B). Comparison of the cross-peak intensities in experiments recorded with and without decoupling yields the $^3J_{HNH\alpha}$ coupling constants.

The signal intensities in the decoupled data set S_d are independent of the $^3J_{HNH\alpha}$ coupling constants, whereas the signal intensities in the J-modulated data set S_m recorded without decoupling depend on the $^3J_{HNH\alpha}$ coupling constants with $\cos(\pi\,^3J_{HNH\alpha}\tau)$, where τ is the time period $4T + 2\Delta$ between the 90°(^1H) pulses in the CT-HMQC-HA experiment (Figure 1A) or the time period $4T + 2\Delta - 4\varepsilon$ in the CT-HMQC-HN experiment (Figure 1B). The experimental coupling constant J_{exp} is determined by the ratio of the cross-peak intensities in the J-modulated (S_m) and decoupled (S_d) spectra by the equation

$$\frac{S_m}{S_d} = \cos(\pi J_{exp}\tau) \qquad (1)$$

Equation 1 shows that no J-evolution times longer than the inverse of the maximum expected coupling constant should be used to avoid ambiguities in the determined coupling constants.

Representative regions of the J-modulated and decoupled spectra of 2D CT-HMQC-HA and 2D CT-

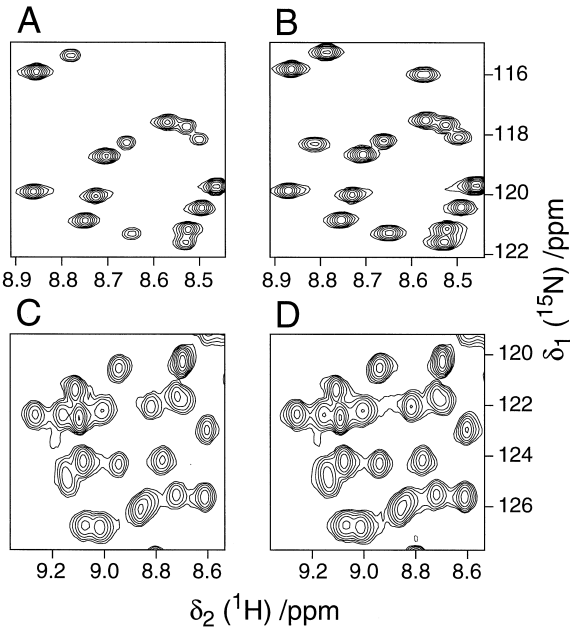

Figure 2. Representative spectral regions from CT-HMQC-HA and CT-HMQC-HN experiments recorded at 600 MHz ^{1}H frequency on a Bruker DMX-600 NMR spectrometer. Contour lines are plotted on a logarithmic scale with a factor of 1.6 between subsequent levels. (A, B) J-modulated and decoupled spectrum, respectively, of a CT-HMQC-HA experiment recorded with a 5.4 mM solution of ^{15}N-labelled N-terminal domain of *E. coli* arginine repressor (ArgR-N, 78 amino acid residues) at pH 5.5, 28 °C. Total recording time 5.5 h. (C, D) J-modulated and decoupled spectrum, respectively, of a CT-HMQC-HN experiment recorded with a 2.1 mM solution of ^{15}N/^{13}C-labelled *E. coli* flavodoxin (176 residues) at pH 6.2, 20 °C. Total recording time 4.5 h.

HMQC-HN experiments recorded with ^{15}N-labelled ArgR-N (Sunnerhagen et al., 1997) and ^{15}N/^{13}C doubly labelled flavodoxin (Ponstingl and Otting, 1997) are shown in Figure 2. To determine the signal intensity ratio S_m/S_d, a small spectral region around each peak maximum was integrated and the same integration region was used for each pair of J-modulated and decoupled spectra. The experimental coupling constants J_{exp} were obtained from Equation 1 and corrected for differential relaxation effects (see below).

The accuracy of the $^{3}J_{HNH\alpha}$ coupling constants measured by the new experiments was assessed by comparison with established experiments. For ArgR-N, coupling constants were determined for 64 out of 72 ^{15}N-^{1}H cross peaks from CT-HMQC-HN and CT-HMQC-HA experiments and compared to the corresponding values determined from fitting the amide proton signals observed in an HSQC spectrum (Szyperski et al., 1992). For flavodoxin, coupling constants were determined for 115 out of 155 ^{15}N-

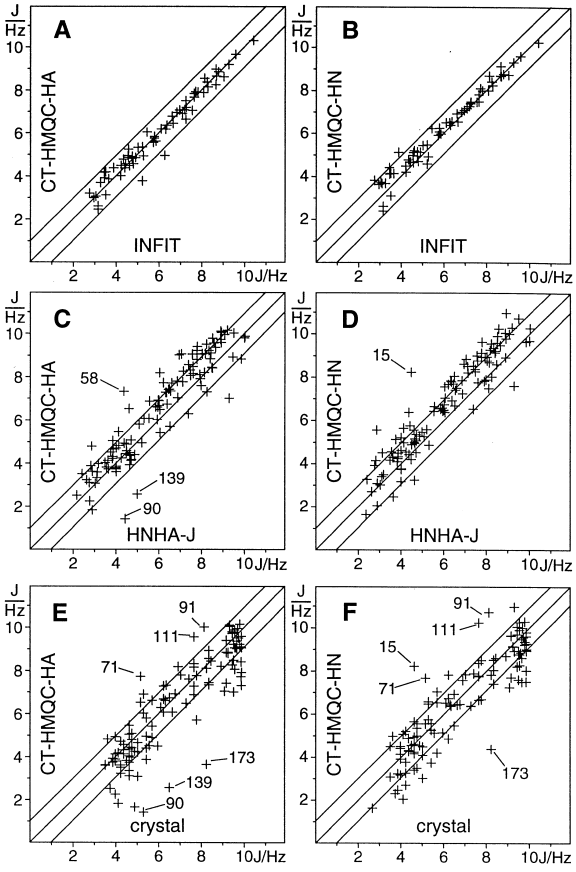

Figure 3. Comparison of $^{3}J_{HNH\alpha}$ coupling constants measured by the CT-HMQC-HA (A, C, E) and CT-HMQC-HN (B, D, F) pulse schemes of Figure 1 with coupling constants obtained by different methods. Lines drawn parallel to the diagonal identify 1 Hz deviations from perfect correlation. (A, B) Coupling constants measured for *E. coli* ArgR-N versus coupling constants determined from the multiplet splittings in a 2D [^{15}N,^{1}H]-HSQC spectrum (total recording time 2 h) using the program INFIT (Szyperski et al., 1992). (C, D) Coupling constants measured for oxidized *E. coli* flavodoxin versus coupling constants measured from ratios of diagonal and cross-peak heights in a 3D HNHA-J (Vuister and Bax, 1993) experiment. The 3D HNHA-J experiment was recorded using the WET sequence (Smallcombe et al., 1995) for water suppression, $2\zeta = 19.26$ ms, $t_{1max}(^{15}N) = 17.7$ ms, $t_{2max}(^{1}H) = 11.5$ ms, $t_{3max}(^{1}H) = 114.7$ ms and a total experimental time of 41.5 h. (E, F) Coupling constants measured for oxidized *E. coli* flavodoxin versus reference values calculated from the crystal structure (Hoover and Ludwig, 1997) using the Karplus curve parametrization of Vuister and Bax (1993). Selected outlayers are labelled by the sequence number of the corresponding residue using the numbering of Ponstingl and Otting (1997). Experimentally measured values were corrected for differential relaxation effects assuming average H^{α} spin-flip rates of 3.8 s^{-1} for ArgR-N and 8.3 s^{-1} for flavodoxin. $\Delta\rho$ values were obtained from 1D NOE experiments, monitoring the decay of the selectively excited H^{α} resonances with increasing mixing times (Stott et al., 1997).

^{1}H cross peaks observed in the CT-HMQC-HA and CT-HMQC-HN experiments and compared to the corresponding values determined from a 3D HNHA-J spectrum and predicted from the crystal structure. The coupling constants measured for ArgR-N by the CT-HMQC-HA and CT-HMQC-HN experiments agree closely with the values measured by line fitting from an HSQC experiment, with no deviation larger than 1.4 Hz (Figures 3A and B). Larger deviations are observed when the $^3J_{HNH\alpha}$ coupling constants measured for flavodoxin by the CT-HMQC-HA and CT-HMQC-HN experiments are compared to corresponding values determined from a 3D HNHA-J experiment (Figures 3C and D). Increased uncertainties in the measurements would be expected due to decreased sensitivity, broader line widths and more frequent partial overlap in the spectra of flavodoxin compared to those of ArgR-N. As noted earlier, the $^3J_{HNH\alpha}$ coupling values from the 3D HNHA-J experiment appear systematically too small (Kuboniwa et al., 1994). The coupling constants measured with the CT-HMQC-HA and CT-HMQC-HN experiments correlated with those predicted by the crystal structure (Hoover and Ludwig, 1997) with rms deviations of 1.29 and 1.10 Hz, respectively (Figures 3E and F). The corresponding rms deviation of the values measured by the 3D HNHA-J experiment was 0.96 Hz, after adding 0.63 Hz to all measured values to compensate for the systematic deviation (Kuboniwa et al., 1994).

Most of the differences observed between experimental $^3J_{HNH\alpha}$ coupling constants and the corresponding values predicted from the crystal structure seem to arise from differences between the crystal and solution structure or from motional averaging in solution. Thus, similar $^3J_{HNH\alpha}$ coupling constants were measured for residues 71, 91, 111 and 173 in the CT-HMQC-HA, CT-HMQC-HN and 3D HNHA-J experiments (Figures 3C and D; the H^α-H^N cross peak of residue 173 was not identified in the 3D HNHA-J spectrum), but quite different values are predicted by the crystal structure. For other residues, a large uncertainty was indicated already by weak cross-peak intensities (residue 15 in the CT-HMQC-HN experiment and residue 58 in the CT-HMQC-HA experiment).

In summary, using comparable t_{1max} values in the ^{15}N dimension of the CT-HMQC-HA, CT-HMQC-HN and 3D HNHA-J experiments, a comparable number of $^3J_{HNH\alpha}$ coupling constants could be measured for flavodoxin by the 2D and 3D experiments. Although the 3D HNHA-J required almost 10 times longer measurement time due to the minimum number of steps in the phase cycle, the rms deviation of the measured versus predicted coupling constants was only little improved compared to the values measured from the 2D spectra. For 19 additional non-glycine residues, H^α-H^N cross peaks were observed in the 3D HNHA-J spectrum, for which the diagonal peaks could not be resolved. Improving the resolution in the ^{15}N dimension would increase the recording time of the 3D HNHA-J experiment much more than for the CT-HMQC-HA or CT-HMQC-HN experiments.

The two experiments are complementary in the sense that, depending on the chemical shift ranges of the protein, it may be easier to invert the H^α resonances than to refocus the H^N resonances in a selective way, or vice versa. In general, the CT-HMQC-HN experiment may be preferred over the CT-HMQC-HA experiment, because insufficient excitation of H^N resonances by the selective pulse is immediately detected by weak intensity of the corresponding cross peaks. Furthermore, too small coupling constants were measured for residues 90 and 139 in the CT-HMQC-HA experiment for an unexplained reason (Figure 3C). In either experiment, if some H^α or H^N resonances are inappropriately excited by the semi-selective decoupling pulses, the corresponding $^3J_{HNH\alpha}$ coupling constants can be measured by further experiments with decoupling pulses at different frequencies, as long as the H^α and H^N resonances can be excited separately.

When relaxation rates approach the magnitude of the scalar couplings, the values measured by any experimental technique deviate from the true coupling constant (Lynden-Bell, 1967; Harbison, 1993; Rexroth et al., 1995). The most important effect on $^3J_{HNH\alpha}$ measurements arises from H^α spin flips, leading to enhanced relaxation of amide proton magnetization which is antiphase with respect to α protons compared to in-phase amide proton magnetization (Boulat and Bodenhausen, 1993; Harbison, 1993). The difference in relaxation rates of the two magnetizations, $\Delta\rho$, is approximately equal to the selective longitudinal relaxation rate $1/T_{1,\alpha}$ of the α proton (Vuister and Bax, 1993).

To calculate the effect of $\Delta\rho$ on the signal intensity ratio S_m/S_d observed in CT-HMQC-HA and CT-HMQC-HN spectra, we disregard the presence of the ^{15}N spins, which are merely used to resolve the spectra in the heteronuclear frequency dimension. The spin operator components of the amide and α protons are denoted as N and A, respectively. Since proton chemical shifts are refocused, it is sufficient to calculate the time evolution of the coefficient i(t) of the

in-phase component N_y, relaxing with rate ρ, and of the coefficient a(t) of the antiphase component $2N_xA_z$, relaxing with rate $\rho + \Delta\rho$, solely with respect to the J-coupling and relaxation. To describe the evolution of the two components i(t) and a(t) with time t for a free precession interval [0, t], the following system of coupled differential equations (Boulat and Bodenhausen, 1993; Harbison, 1993; Norwood, 1993; Kuboniwa et al., 1994) has to be integrated:

$$d\begin{pmatrix} i(t) \\ a(t) \end{pmatrix} = \begin{pmatrix} -\rho & \pi J_{true} \\ -\pi J_{true} & -(\rho + \Delta\rho) \end{pmatrix} \begin{pmatrix} i(t) \\ a(t) \end{pmatrix} dt \quad (2)$$

where J_{true} is the true coupling constant that would be observed if relaxation could be neglected. Denoting the coefficients at time $t = 0$ by i_0 and a_0, and introducing $\eta = \Delta\rho/(2\pi J_{true})$, the following solution is obtained for $0 \leq \eta < 1$:

$$i(t) = \left[i_0 \left(\cos(\pi J_{scal} t) + \frac{\eta}{\sqrt{1-\eta^2}} \sin(\pi J_{scal} t) \right) + a_0 \frac{1}{\sqrt{1-\eta^2}} \sin(\pi J_{scal} t) \right] \exp\left[-\left(\rho + \frac{\Delta\rho}{2} \right) t \right] \quad (3a)$$

$$a(t) = \left[a_0 \left(\cos(\pi J_{scal} t) - \frac{\eta}{\sqrt{1-\eta^2}} \sin(\pi J_{scal} t) \right) - i_0 \frac{1}{\sqrt{1-\eta^2}} \sin(\pi J_{scal} t) \right] \exp\left[-\left(\rho + \frac{\Delta\rho}{2} \right) t \right] \quad (3b)$$

with

$$J_{scal} = J_{true}\sqrt{1-\eta^2} \quad (4)$$

The differential relaxation effects were calculated by considering the pulse schemes of Figure 1 as a sequence of free-precession intervals separated by ideal instantaneous pulses. Starting from $(i_0, a_0) = (-1, 0)$ after the initial $90^\circ_x(^1H)$ pulse, Eqs. 3a and 3b were applied for each free precession interval. Only the in-phase component was retained after the final $90^\circ_y(^1H)$ purge pulse. The action of a semi-selective 180° pulse of duration τ_p was approximated by the sequence $[\tau_p/2 - 180^\circ_x - \tau_p/2]$, where the 180°_x pulse was assumed to be infinitely short yet selective for α or amide protons, respectively.

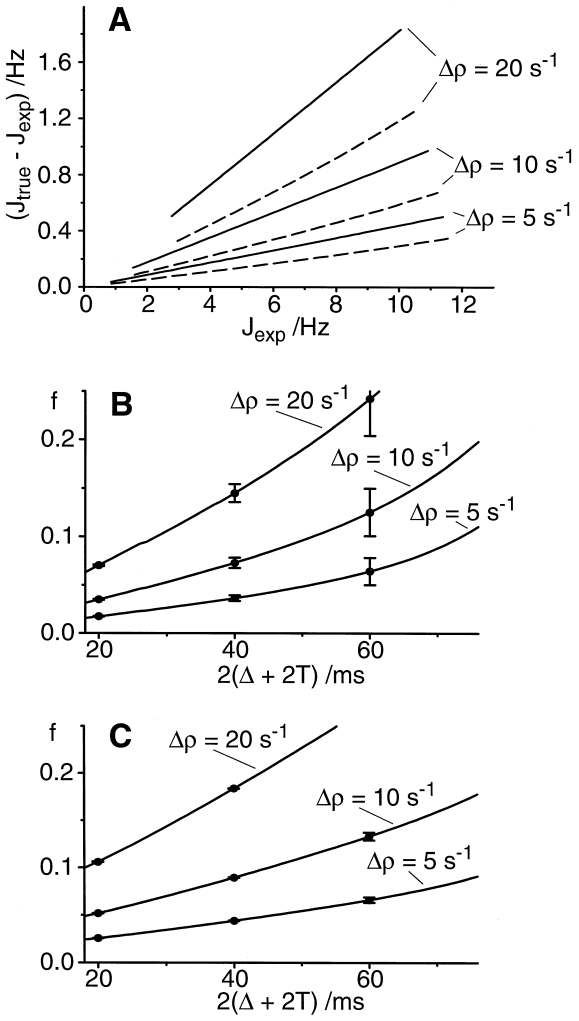

Figure 4. Correction of experimental $^3J_{HNH\alpha}$ coupling constants for differential relaxation. (A) Deviation of the true coupling constant J_{true} from the measured value J_{exp}. The difference $J_{true} - J_{exp}$ was calculated for differences $\Delta\rho$ between in-phase and antiphase relaxation rates of 5, 10 and 20 s^{-1}. The correction curves are not valid for $J_{true} < \Delta\rho/(2\pi)$ which would violate the condition $\eta < 1$ (Eq. 4). Dashed line: correction for J_{exp} values measured by the CT-HMQC-HA experiment based on Eq. 1 using $4T + 2\Delta = 32.4$ ms and neglecting the influence of the decoupling pulse train on the relaxation rate of the α protons (Hajduk et al., 1993); Continuous line: correction for J_{exp} measured by the CT-HMQC-HN experiment using Eq. 1 with $\varepsilon = 1.75$ ms and $4T + 2\Delta = 40.4$ ms. (B, C) Plots of the correction term f, which can be used with the relation $J_{true} = (1 + f)J_{exp}$, as a function of $4T + 2\Delta$ (Figure 1) and the difference in relaxation rates of in-phase and antiphase magnetization $\Delta\rho$. Vertical bars indicate the maximum error made by assuming that f is constant over the range $\Delta\rho/(2\pi) < J_{true} < 12.0$ Hz. (B) Correction for CT-HMQC-HA data. The duration τ_p of the semi-selective pulses was adjusted so that $(2T + \Delta)/\tau_p$ was an integral number and $\tau_p \cong 5.4$ ms. (C) Correction for CT-HMQC-HN data, with $\varepsilon = 2$ ms (Figure 1B).

The exponential factors of Eqs. 3a and 3b cancel in the calculation of the signal intensity ratio S_m/S_d. In principle, different relaxation rates $\Delta\rho$ may be expected for the decoupled and J-modulated recordings of the CT-HMQC-HA experiment, because the semi-selective inversion pulses applied to the α protons transiently convert antiphase magnetization into two-spin coherence (Hajduk et al., 1993). However, this effect is small, because the generation of antiphase magnetization is restricted by the decoupling.

Given the magnitude of $\Delta\rho$, the expected signal intensity ratios S_m/S_d were calculated for a range of J_{true} values and were used to calculate the corresponding experimental coupling constants J_{exp} (Eq. 1). The difference $J_{true} - J_{exp}$ is in good approximation proportional to J_{exp} with a factor $f \cong (J_{true} - J_{exp})/J_{exp}$ (Figure 4A). f is characteristic for the experiment type and depends on $\Delta\rho$ and the delay settings used. Similarly, Eq. 3 was used to calculate f values to correct the coupling constant values measured from 3D HNHA-J experiments. If small dispersive antiphase contributions (Harbison, 1993) are neglected, $^3J_{HNH\alpha}$ values extracted by line fitting from in-phase $^1H^N$ doublets correspond to J_{scal} which can be corrected for differential relaxation effects using Eq. 4. The magnitude of the correction decreases with increasing coupling constants. For the smallest J_{scal} value (2.68 Hz) measured by line fitting for ArgR-N, the correction term $J_{true} - J_{scal}$ was calculated to be 0.07 Hz. Figure 4 shows pictorial representations of the correction terms for the CT-HMQC-HA and CT-HMQC-HN experiments.

Acknowledgements

The authors thank Prof. Martha L. Ludwig for a preprint and the coordinates of the crystal structure of oxidized *E. coli* flavodoxin and Dr. Maria Sunnerhagen for providing the NMR samples of the arginine-repressor domain. This work was supported by the Swedish Natural Science Research Council (project 10161). H.P. acknowledges a graduate student stipend from the EU training and mobility programme (BIO4CT965011).

References

Billeter, M., Neri, D., Otting, G., Qian, Y.Q. and Wüthrich, K. (1992) *J. Biomol. NMR*, **2**, 257–274.

Boulat, B. and Bodenhausen, G. (1993) *J. Biomol. NMR*, **3**, 335–348.

Frey, M.H., Wagner, G., Vašák, M., Sørensen, O.W., Neuhaus, D., Wörgötter, E., Kägi, J.H.R., Ernst, R.R. and Wüthrich, K. (1985) *J. Am. Chem. Soc.*, **107**, 6847–6851.

Geen, H. and Freeman, R. (1991) *J. Magn. Reson.*, **93**, 93–141.

Görlach, M., Wittekind, M., Farmer II, B.T., Kay, L.E. and Mueller, L. (1993) *J. Magn. Reson.*, **B101**, 194–197.

Hajduk, P.J., Horita, D.A. and Lerner, L.E. (1993) *J. Magn. Reson.*, **A103**, 40–52.

Harbison, G.S. (1993) *J. Am. Chem. Soc.*, **115**, 3026–3027.

Hoover, D.M. and Ludwig, M.L. (1997) *Protein Sci.*, **6**, 2525–2537.

Kay, L.E., Brooks, B., Sparks, S.W., Torchia, D.A. and Bax, A. (1989) *J. Am. Chem. Soc.*, **111**, 5488–5490.

Kuboniwa, H., Grzesiek, S., Delaglio, F. and Bax, A. (1994) *J. Biomol. NMR*, **4**, 871–878.

Löhr, F. and Rüterjans, H. (1995) *J. Biomol. NMR*, **5**, 25–36.

Lynden-Bell, R.M. (1967) *Prog. NMR Spectrosc.*, **2**, 163–204.

Madsen, J.C., Sørensen, O.W., Sørensen, P. and Poulsen, F.M. (1993) *J. Biomol. NMR*, **3**, 239–244.

Marion, D., Ikura, M., Tschudin, R. and Bax, A. (1989) *J. Magn. Reson.*, **85**, 393–399.

Meissner, A., Duus, J. Ø. and Sørensen, O.W. (1997) *J. Magn. Reson.*, **128**, 92–97.

Norwood, T.J. (1993) *J. Magn. Reson.*, **A101**, 109–112.

Ponstingl, H. and Otting, G. (1997) *Eur. J. Biochem.*, **244**, 384–399.

Rexroth, A., Schmidt, P., Szalma, S., Geppert, T., Schwalbe, H. and Griesinger, C. (1995) *J. Am. Chem. Soc.*, **117**, 10389–10390.

Schmieder, P., Thanabal, V., McIntosh, L.P., Dahlquist, F.W. and Wagner, G. (1991) *J. Am. Chem. Soc.*, **113**, 6323–6324.

Seip, S., Balbach, J. and Kessler, H. (1992) *Angew. Chem.*, **104**, 1656–1658.

Silver, M.S., Joseph, R.I. and Hoult, D.I. (1984) *J. Magn. Reson.*, **59**, 347–351.

Smallcombe, S.H., Patt, S.L. and Keifer, P.A. (1995) *J. Magn. Reson.*, **A117**, 295–303.

Stott, K., Keeler, J., Van, Q.N. and Shaka, A.J. (1997) *J. Magn. Reson.*, **125**, 302–324.

Sunnerhagen, M., Nilges, M., Otting, G. and Carey, J. (1997) *Nat. Struct. Biol.*, **4**, 819–826.

Sørensen, M.D., Meissner, A. and Sørensen, O.W. (1997) *J. Biomol. NMR*, **10**, 181–186.

Szyperski, T., Güntert, P., Otting, G. and Wüthrich, K. (1992) *J. Magn. Reson.*, **99**, 552–560.

Vuister, G.W. and Bax, A. (1993) *J. Am. Chem. Soc.*, **115**, 7772–7777.

Weisemann, R., Rüterjans, H., Schwalbe, H., Schleucher, J., Bermel, W. and Griesinger, C. (1994) *J. Biomol. NMR*, **4**, 231–240.